

IN SILICO DISCOVERY OF HUMAN AURORA B KINASE INHIBITORS BY MOLECULAR DOCKING, PHARMACOPHORE VALIDATION AND ABSORPTION, DISTRIBUTION, METABOLISM, EXCRETION AND TOXICITY STUDIES

RAJASHEKAR VADLAKONDA^{1*}, SREENIVAS ENAGANTI², RAGHUNANDAN NERELLA³

¹Department of Pharmaceutical Chemistry, Vikas College of Pharmacy, Jangaon, Warangal, Telangana, India. ²Department of Bioinformatics, Averinbiotech, 208, 2nd Floor, Windsor Plaza, Nallakunta, Hyderabad, Telangana, India. ³Department of Pharmaceutical Chemistry, Balaji Institute of Pharmaceutical Sciences, Laknepally, Narsampet, Warangal, Telangana, India.
Email: mailme2rajashekar@gmail.com

Received: 31 August 2016, Revised and Accepted: 22 November 2016

ABSTRACT

Objectives: To predict the anticancer potentiality of some newly designed azaindole derivatives against human Aurora B kinase and to identify the critical features important for their activity.

Methods: Initially, the derivatives of azaindoles, (Z)-2-(oxo-1 H-pyrrolo [2,3-b] pyridine-3 (2H)-ylidene)-N-(p-substituted) hydrazine carbothioamide (scaffold A), (E)-3-((E)-substituted benzylidene hydrazono)-1H-pyrrolo[2,3-b]pyridine-2(3H)-one (scaffold B), and 1-(2-substituted acetyl)-1H-pyrrolo [2,3-b]pyridine-2,3-dione are synthesized and sketched using ACD/ChemSketch (12.0). With the 3D converted compounds, docking into the active site of the retrieved protein Aurora B kinase is carried out using LibDock module of discovery studio (DS). Further absorption, distribution, metabolism, excretion and toxicity (ADMET) properties, ligand, and structure-based pharmacophore modeling are applied using DS.

Results: Through docking and pharmacophore studies, it is revealed that compound C13 (N-((Z)-2-[4-(dimethylamino)phenyl]ethenyl)-1H-pyrrolo[2,3-b]pyridine-3-carboxamide) shows the highest binding affinity and good pharmacophoric features with acceptable fit values of both ligand and structure-based pharmacophore models. Furthermore, the calculated ADMET properties are reliable.

Conclusion: These studies suggest that the compound C13 (N-((Z)-2-[4-(dimethylamino)phenyl]ethenyl)-1H-pyrrolo[2,3-b]pyridine-3-carboxamide) may act as a potent target in the anticancer therapy.

Keywords: Aneuploidy, Aurora B kinase, Azaindole, Cancer, Cell cycle, Genome stability.

© 2017 The Authors. Published by Innovare Academic Sciences Pvt Ltd. This is an open access article under the CC BY license (<http://creativecommons.org/licenses/by/4.0/>) DOI: <http://dx.doi.org/10.22159/ajpcr.2017.v10i2.14974>

INTRODUCTION

Aurora kinases with their interference in various aspects of underlying cell cycle mitotic events, over expressions in malignancy and interference with tumor suppressor and oncogenic signaling pathways, they have arisen as encouraging chemotherapeutic targets for cancer and many diseases accompanied by their deregulation [1-3]. Aurora's are a family of well homologous serine-threonine protein kinases that play an important role in controlling a series of activities at different stages from G2 to cytokinesis during cell division through which normal cell cycle mitosis is maintained [4-6]. The mitotic regulation is necessary for equal and accurate chromosomal segregation to daughter cells during cell division and is of great consequence to preserve genome stability and prevent aneuploidy [7-9]. Hence, any perturbations of the Aurora kinases disorganize mitotic processes leading to chromosomal instability and aneuploidy that is commonly observed in many human cancer cells, which is evident by chromosome loss, translocation and aberrant centrosome duplication, indicating an underlying deregulation in chromosome segregation, centrosome duplication and segregation [8-10]. In particular, this critical activity of Aurora kinases put forward that their blockage may result in arrest of the cell cycle in cancer cells that have been of intense research in identifying distinctive Aurora kinase inhibitors as probable lead molecules for cancer [11,12].

Aurora B kinase is a member of Aurora family, found as a catalytic part of the four-subunit chromosomal passenger complex (CPC) along with INCENP, Survivin and Borealin which are codependent for stability and localization [13-15]. These proteins share a characteristic pattern of

association with chromatin in prophase, centromeres in metaphase and early anaphase, and then the midzone and midbody in late anaphase and telophase, respectively [16-18]. This differential localization of the CPC throughout mitosis suggested that this complex ensures the effective and spatially restricted phosphorylation of substrates involved in chromosome condensation, correction of erroneous kinetochore-microtubule attachments, activation of the spindle assembly checkpoint (SAC), and constructs contractile apparatus during cytokinesis. Given the critical and diverse roles of Aurora B in mitosis and cytokinesis, its cellular functions require proper regulation by inducing autophosphorylation through several mechanisms and controlled interactions with its substrates. Knockdown of any member of the complex delocalizes the others where Aurora B activity is diminished disrupts mitotic progression that might correlate with aneuploidy which continues to the formation of an abnormal nuclear morphology in cancer cells [19-24]. Therefore, modulations of these altered mechanisms through the inhibition of Aurora B kinase is considered as a therapeutic strategy in many cancers where it contribute its role in proper cell cycle events leading to mitotic progression associated with genome stability.

In this study, we have investigated the anticancer activity of synthetic derivatives of azaindole against Aurora B kinase through docking, pharmacophore and absorption, distribution, metabolism, excretion and toxicity (ADMET) studies. The overall results obtained from this study reveal that these compounds would aid in designing new lead molecules in cancer therapy.

Chemistry

A series of azaindole derivatives, (Z)-2-(oxo-1H-pyrrolo [2,3-b]pyridine-3(2H)-ylidene)-N-(p-substituted) hydrazine carbothioamide (scaffold A), (E)-3-((E)-substituted benzylidene hydrazono)-1H-pyrrolo[2,3-b]pyridine-2(3H)-one (scaffold B), and 1-(2-substituted acetyl)-1H-pyrrolo [2,3-b]pyridine-2,3-dione are synthesized schematically. The synthetic pathway for the synthesis of our targeted compounds is illustrated in Scheme 1. Fig. 1 shows the chemical structures of the scaffolds. The derivatives of the scaffolds with different substitutions in the R position, their IUPAC names, molecular formula and molecular weight are tabulated in Table 1.

METHODS

Protein preparation

The structure of human Aurora B Kinase (PDB: 4AF3) complexed with VX-680 and INCENP is retrieved from the PDB database having a resolution of 2.75 Å. After importing into the discovery studio 2.5 (DS), using the clean Protein protocol, the protein is prepared for correcting the lack of hydrogen atoms, missing atoms and residues, incorrect atom order in amino acids, protonation states of ionizable side chains and terminal groups using predicted pKs, to complete the protein chain. Water molecules and all the heteroatoms are removed, and CHARMM force field is applied for energy minimization using different algorithms till the protein reaches a convergence

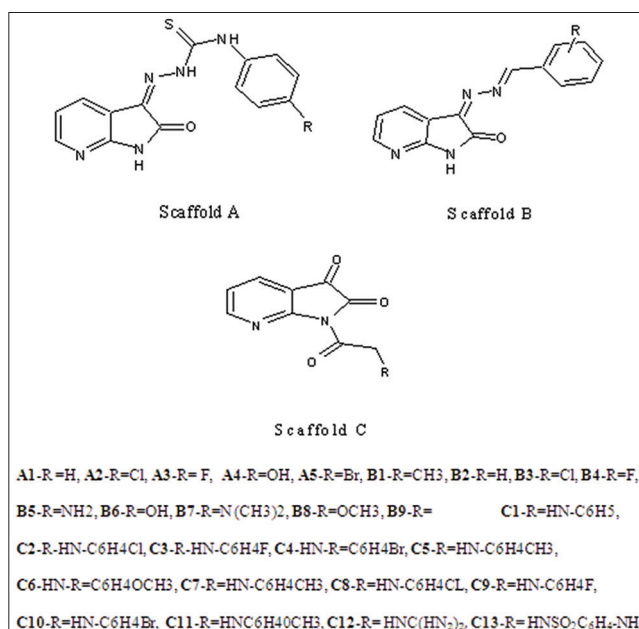
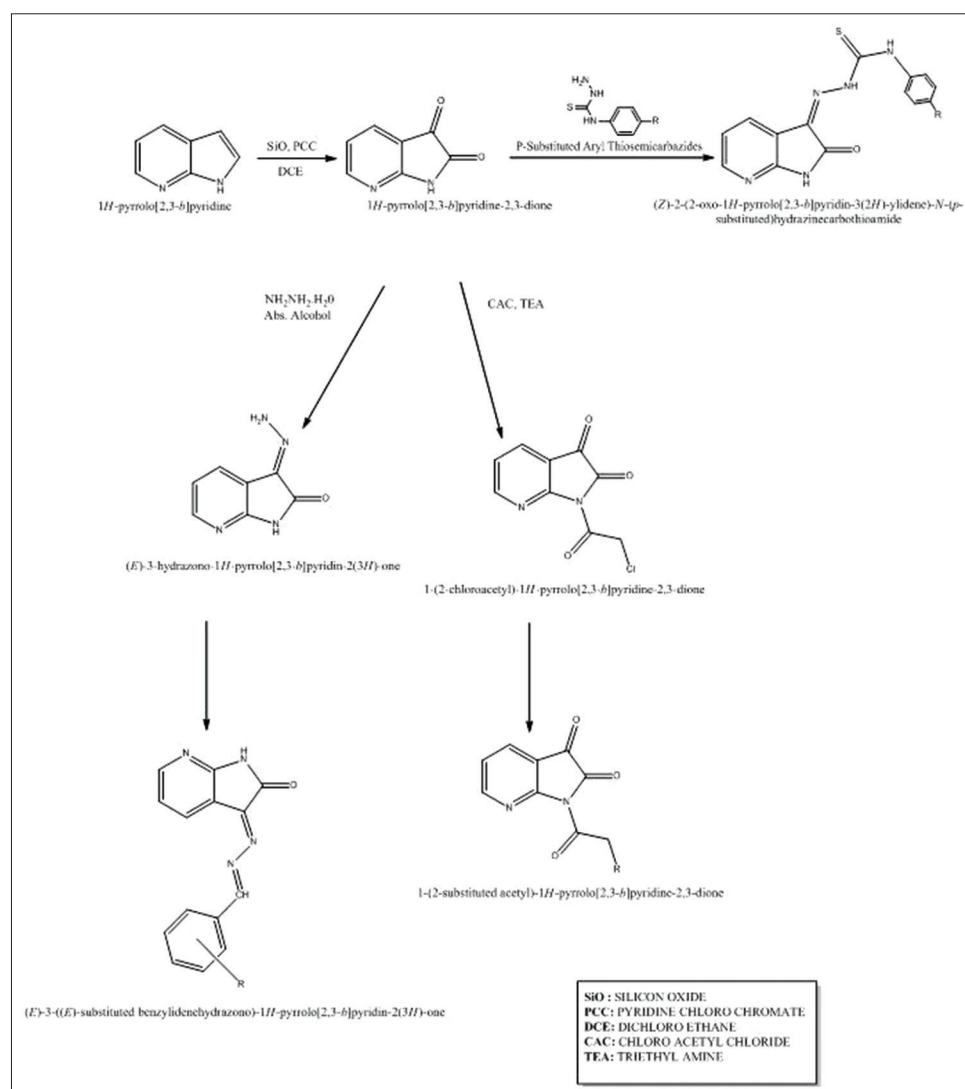


Fig. 1: Chemical structure of the scaffolds a-c



Scheme 1: Synthetic pathway for azaindole derivatives

Table 1: Molecular properties of the azaindole derivatives

Compound	R	Molecular formula	Molecular weight	IUPAC name
A1	H	C ₁₄ H ₁₁ N ₅ OS	297.33504	(2Z)-2-(2-oxo-1,2-dihydro-3H-pyrrolo[2,3-b]pyridin-3-ylidene)-N-phenylhydrazine carbothioamide
A2	Cl	C ₁₄ H ₁₀ ClN ₅ OS	331.7801	(2Z)-N-(4-chlorophenyl)-2-(2-oxo-1,2-dihydro-3H-pyrrolo[2,3-b]pyridin-3-ylidene) hydrazine carbothioamide
A3	F	C ₁₄ H ₁₀ FN ₅ OS	315.3255032	(2Z)-N-(4-fluorophenyl)-2-(2-oxo-1,2-dihydro-3H-pyrrolo[2,3-b]pyridin-3-ylidene) hydrazine carbothioamide
A4	OH	C ₁₄ H ₁₁ N ₅ O ₂ S	313.33444	(2Z)-N-(4-hydroxyphenyl)-2-(2-oxo-1,2-dihydro-3H-pyrrolo[2,3-b]pyridin-3-ylidene) hydrazine carbothioamide
A5	Br	C ₁₄ H ₁₀ BrN ₅ OS	376.2311	(2Z)-N-(4-bromophenyl)-2-(2-oxo-1,2-dihydro-3H-pyrrolo[2,3-b]pyridin-3-ylidene) hydrazine carbothioamide
B1	CH ₃	C ₁₅ H ₁₂ N ₄ O	264.28198	(3Z)-3-[(2E)-(4-methylbenzylidene)hydrazinylidene]-1,3-dihydro-2H-pyrrolo[2,3-b]pyridin-2-one
B2	H	C ₁₄ H ₁₀ N ₄ O	250.2554	(3Z)-3-[(2E)-benzylidenehydrazinylidene]-1,3-dihydro-2H-pyrrolo[2,3-b]pyridin-2-one
B3	Cl	C ₁₄ H ₉ ClN ₄ O	284.70046	(3Z)-3-[(2E)-(4-chlorobenzylidene)hydrazinylidene]-1,3-dihydro-2H-pyrrolo[2,3-b]pyridin-2-one
B4	F	C ₁₄ H ₉ FN ₄ O	268.2458632	(3Z)-3-[(2E)-(4-fluorobenzylidene)hydrazinylidene]-1,3-dihydro-2H-pyrrolo[2,3-b]pyridin-2-one
B5	NH ₂	C ₁₄ H ₁₁ N ₅ O	265.27004	(3Z)-3-[(2E)-(4-aminobenzylidene)hydrazinylidene]-1,3-dihydro-2H-pyrrolo[2,3-b]pyridin-2-one
B6	OH	C ₁₄ H ₁₀ N ₄ O ₂	266.2548	(3Z)-3-[(2E)-(4-hydroxybenzylidene)hydrazinylidene]-1,3-dihydro-2H-pyrrolo[2,3-b]pyridin-2-one
B7	N(CH ₃) ₂	C ₁₆ H ₁₅ N ₅ O	293.3232	(3Z)-3-[(2E)-[4-(dimethylamino)benzylidene]hydrazinylidene]-1,3-dihydro-2H-pyrrolo[2,3-b]pyridin-2-one
B8	OCH ₃	C ₁₅ H ₁₂ N ₄ O ₂	280.28138	(3Z)-3-[(2E)-(4-methoxybenzylidene)hydrazinylidene]-1,3-dihydro-2H-pyrrolo[2,3-b]pyridin-2-one
B9		C ₁₆ H ₁₂ N ₄ O	276.29268	(3Z)-3-[(2E)-[2-phenylprop-2-en-1-ylidene]hydrazinylidene]-1,3-dihydro-2H-pyrrolo[2,3-b]pyridin-2-one
C1	HN-C ₆ H ₅	C ₁₅ H ₁₁ N ₃ O ₃	281.26614	1-[(phenylamino)acetyl]-1H-pyrrolo[2,3-b]pyridine-2,3-dione
C2	HN-C ₆ H ₄ Cl	C ₁₅ H ₁₀ ClN ₃ O ₃	315.7112	1-[[4-chlorophenyl]amino]acetyl]-1H-pyrrolo[2,3-b]pyridine-2,3-dione
C3	HN-C ₆ H ₄ F	C ₁₅ H ₁₀ FN ₃ O ₃	299.2566032	1-[[4-fluorophenyl]amino]acetyl]-1H-pyrrolo[2,3-b]pyridine-2,3-dione
C4	HN-C ₆ H ₄ Br	C ₁₅ H ₁₀ BrN ₃ O ₃	360.1622	1-[[4-bromophenyl]amino]acetyl]-1H-pyrrolo[2,3-b]pyridine-2,3-dione
C5	HN-C ₆ H ₄ CH ₃	C ₁₆ H ₁₃ N ₃ O ₃	295.29272	1-[[4-methylphenyl]amino]acetyl]-1H-pyrrolo[2,3-b]pyridine-2,3-dione
C6	HN-C ₆ H ₄ OCH ₃	C ₁₆ H ₁₃ N ₃ O ₄	311.29212	1-[[4-methoxyphenyl]amino]acetyl]-1H-pyrrolo[2,3-b]pyridine-2,3-dione
C7	HN-C ₆ H ₄ CH ₃	C ₁₆ H ₁₃ N ₃ O ₃	295.29272	1-[[2-methylphenyl]amino]acetyl]-1H-pyrrolo[2,3-b]pyridine-2,3-dione
C8	HN-C ₆ H ₄ Cl	C ₁₅ H ₁₀ N ₃ O ₃	315.7112	1-[[2-chlorophenyl]amino]acetyl]-1H-pyrrolo[2,3-b]pyridine-2,3-dione
C9	HN-C ₆ H ₄ F	C ₁₅ H ₁₀ FN ₃ O ₃	299.2566032	1-[[2-fluorophenyl]amino]acetyl]-1H-pyrrolo[2,3-b]pyridine-2,3-dione
C10	HN-C ₆ H ₄ Br	C ₁₅ H ₁₀ BrN ₃ O ₃	360.1622	1-[[2-bromophenyl]amino]acetyl]-1H-pyrrolo[2,3-b]pyridine-2,3-dione
C11	HN-C ₆ H ₄ OCH ₃	C ₁₆ H ₁₃ N ₃ O ₄	311.29212	1-[[2-methoxyphenyl]amino]acetyl]-1H-pyrrolo[2,3-b]pyridine-2,3-dione
C12	HNC(HN ₂) ₂	C ₁₀ H ₉ N ₅ O ₃	247.21016	1-[2-(2,3-dioxo-2,3-dihydro-1H-pyrrolo[2,3-b]pyridin-1-yl)-2-oxoethyl]guanidine
C13	HNSO ₂ C ₆ H ₄ -NH ₂	C ₁₅ H ₁₂ N ₄ O ₅ S	360.34458	4-amino-N-[2-(2,3-dioxo-2,3-dihydro-1H-pyrrolo[2,3-b]pyridin-1-yl)-2-oxoethyl]benzene sulfonamide

gradient 0.001 kcal/mol. Fig. 2 shows the human Aurora B Kinase crystal structure.

Ligand generation and optimization

Using ACD/ChemSketch (12.0), the 2D structures of all the compounds are drawn and saved in mol file format. These saved compounds are later imported into DS and ligand preparation with constraint parameters such as consistency of ionization states, tautomer and isomer generation, removal of duplicate structures, conversion of 2D to 3D structures using catalyst algorithm is done and are energy minimized until the convergence gradient of 0.001 kcal/mol is reached. Fig. 3 shows the 3D structure of the compounds.

Define binding site

Using define and edit binding site tools in DS, the binding site of the human Aurora B Kinase is determined based on the occupied volume of the known ligand VX-680 in the active site. The ligand is first selected, and a sphere is created around the residues comprising binding site at a radius of 9 Å using define sphere from the selection option.

Docking studies

For accurate docking of our compounds into active site of the protein, molecular docking is carried out through site-featured docking

algorithm Libdock module in DS. The binding site features, "HotSpots" are resolved with a grid fixed in active site which counts the hotspot map for polar and a polar cluster and further used for the alignment of the ligand conformations to the protein interaction sites. Finally, it returns all the minimized ligand poses and based on the high LibDock score; each pose is assessed for estimating binding energies and the protein-complex pose with the best binding energy is used for further binding mode analysis.

Pharmacophore model generation and validation

Two different methods are applied for the pharmacophore model generation using DS Catalyst: Ligand (common feature approach) and structure-based pharmacophore modeling, to analyze the fitting of the designed compounds to the generated pharmacophores.

Ligand-based pharmacophore modeling

Using HipHop algorithm in DS, Common feature pharmacophore modeling is applied with synthesized inhibitors of our target protein Aurora B kinase, which takes advantage of the chemical features commonly observed in the active compounds for the pharmacophore generation. Using DS diverse conformation generation module, a maximum of 255 conformations are created per compound using FAST Conformer method within an energy range 20 kcal/mol over the global

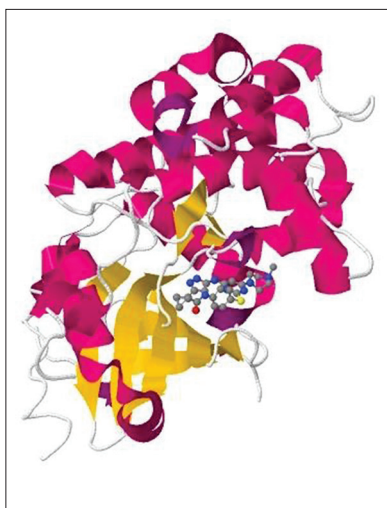


Fig. 2: The structure of human Aurora B Kinase (PDB ID:4AF3) complexed with VX-680

energy minimum. All the possible pharmacophore feature mappings with desired chemical groups are identified with Feature Mapping module and common feature pharmacophore generation protocol is executed including the features like, hydrogen bond donor (HBD), hydrogen bond acceptor (HBA), hydrophobic (HY), ring aromatic (RA), and positive ionizable (P) with principal value as "2," maximum omit feature value as "0" and minimum inter-feature distance as "2.97 Å." 10 pharmacophore hypotheses are generated preferring the best one with high ranking score which further analyzed for compound mapping. The best-mapped compound is chosen based on the fit values and aligned pharmacophoric features.

Structure-based pharmacophore modeling

To further identify the critical structural features of our target protein Aurora B kinase, structure-based pharmacophore modeling is employed utilizing the current knowledge of the protein - ligand interactions. To construct a pharmacophore model, corresponding possible interaction points from the protein's active site is computed using DS 'Interaction Generation' protocol. The active site is then analyzed for HBD, acceptors, and HY features by generating pharmacophore query from the Ludi interaction maps. The maximum

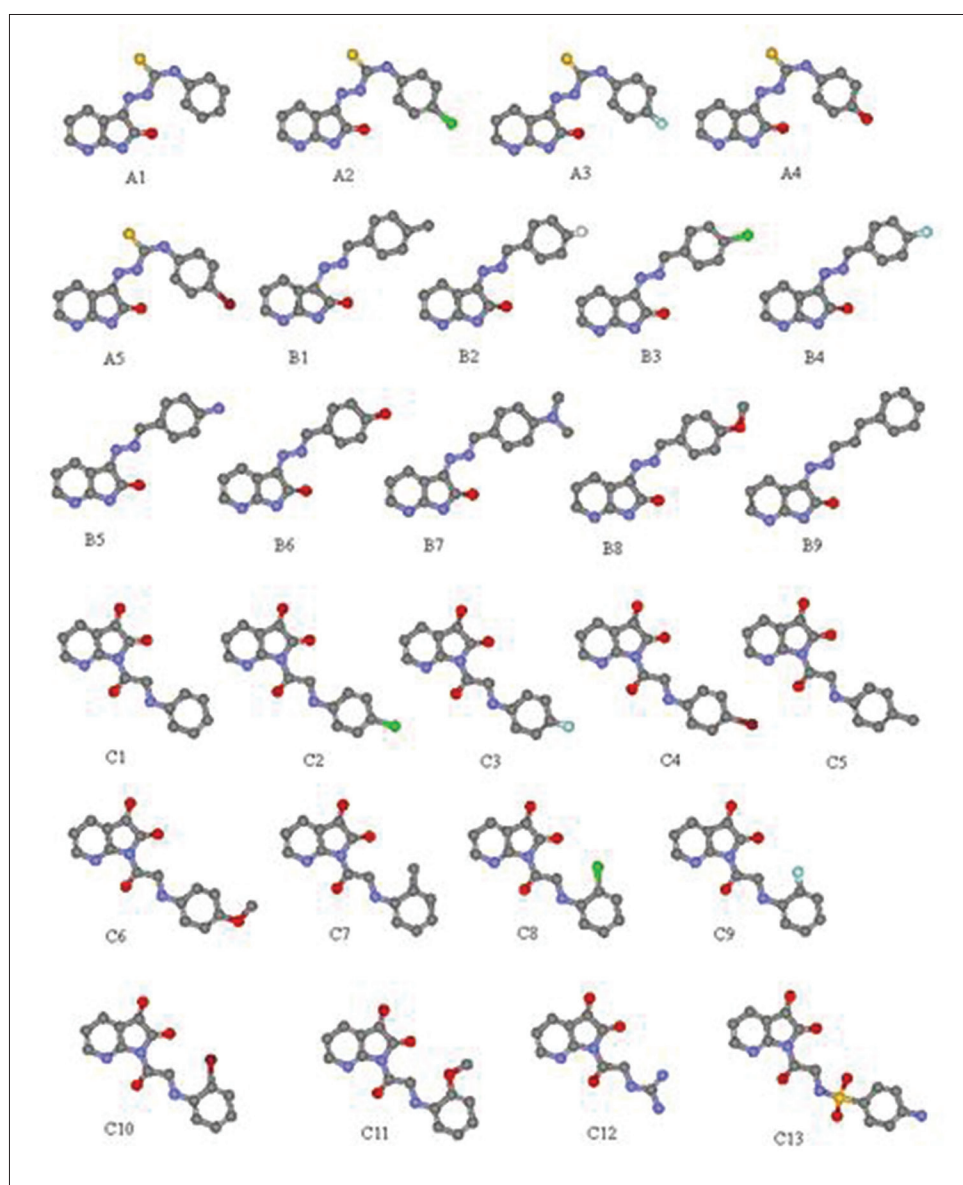


Fig. 3: 3D structures of the compounds

and minimum features are set to 2 and 1, respectively. The selected features are then clustered using edit and cluster pharmacophores tool, and a structure-based pharmacophore model is generated which further validated according to the compounds orientation in the active site using DS ligand pharmacophore mapping protocol with best flexible search option and maximum omitted features as 2. The predictive ability of the model was analyzed based on the best-fit values that signify how well the compounds are fitted onto the pharmacophoric features.

ADMET studies

ADMET analysis is performed using DS ADMET descriptors protocol to derive the drug likeliness properties of the synthesized compounds which include absorption, blood-brain barrier (BBB), aqueous solubility, hepatotoxicity, plasma protein binding (PPB), and cytochrome P450 (CYP) 2D6 probability enzyme inhibition study. Results are analyzed according to the DS standard parameters.

RESULTS AND DISCUSSION

Docking studies

Docking studies carried out using LibDock is used to analyze binding modes and affinities of the compounds with human Aurora B kinase (PDB:4AF3). Of all the conformations generated for each compound, the compound with the highest LibDock score is taken for interaction analysis of the hydrogen bonding. LibDock scores of all the compounds along with their hydrogen bond interactions and bond lengths are depicted in Table 2. From the overall docking and interaction analysis, the best conformation of the compound C13 docked complex shows

high LibDock score of 116.558 kcal/mol and forms three hydrogen bonds with the protein Aurora B kinase (Fig. 4).

Pharmacophore modeling and validation

Ligand-based pharmacophore modeling

The HipHop algorithm computes ten common pharmacophore hypotheses with their ranking scores ranging from 266.453 to 249.195 (Table 3), and hypothesis 1 is considered as the most reliable pharmacophore hypothesis (Fig. 5a) containing three HBD and one RA feature. All the compounds are mapped on to the hypothesis 1, ranked according to their fit values (Table 4) and the compound C13 fitted well on the pharmacophore with a high fit value of 4.093 (Fig. 5b).

Structure-based pharmacophore modeling

The Interaction Generation protocol constructed a structured-based pharmacophore model of our protein human Aurora B Kinase based on the active site residues inside the sphere. The final edited pharmacophore model has two HBD, two HBA, and two HY features (Fig. 6a). Using ligand pharmacophore mapping, compounds are mapped and ranked according to the fit values (Table 5). Based on the fit values, the compound C13 fitted well on the pharmacophore with a fit value of 3.159 (Fig. 6b).

ADMET studies

The compounds are further examined by their pharmacokinetic and toxicity studies using ADMET descriptors analysis protocol in DS. Using the standards provided by DS, the results are analyzed. The calculated parameters are tabulated in Table 6. According to the DS parameters,

Table 2: Summary of docking information of the top ranked poses of the compounds (A-1 to A-5, B-1 to B-9 and C1-C13) with Human Aurora B Kinase (PDB ID: 4AF3)

Name	Electrostatic energy	Van der waals energy	LibDock score	Interacting aminoacids	Interacting atoms	h-bond distance
A1	-9.68	2.931	92.332	LEU83, LYS106 LEU207 Pro158, Leu207, Tyr156 Glu155.Ala104, Ala157	No hydrogen bonds	
A2	-13.871	4.141	99.436	LEU83 LYS106 LEU207 Pro158, Leu207, Tyr156 Glu155.Ala104, Ala157	A2:H26 - A: LEU83:O A2:H26 - A: LEU83:C A2:H30 - A: LYS106:CD A2:H30 - A: LYS106:HD1 A2:H30 - A: LYS106:HD2	2.255000 2.208000 1.844000 1.767000 1.338000
A3	-16.838	3.549	100.033	LEU83 LYS106 LEU207 Pro158, Leu207, Tyr156 Glu155.Ala104, Ala157	A3:H26 - A: LEU83:O A3:H26 - A: LEU83:C A3:H29 - A: LYS106:CD A3:H29 - A: LYS106:HD2	2.409000 2.176000 1.943000 1.261000
A4	-25.147	1.765	99.937	LEU83 LYS106 LEU207 Pro158, Leu207, Tyr156 Glu155.Ala104, Ala157	A4:H26 - A: LEU83:O	2.304000
A5	-11.207	3.142	99.646	LEU83 LYS106 LEU207 Pro158, Leu207, Tyr156 Glu155.Ala104, Ala157	A5:H26 - A: LEU83:O A5:C17 - A: LYS106:H22 A5:H29 - A: LYS106:CD A5:H29 - A: LYS106:HD2	2.298000 2.199000 1.869000 1.380000
B1	-12.703	3.562	89.397	Pro158, Leu207, Tyr156 Glu155.Ala104, Ala157	No ligand interaction atoms	

(Contd...)

Table 2: (Continued)

Name	Electrostatic energy	Van der waals energy	LibDock score	Interacting aminoacids	Interacting atoms	h-bond distance	
B2	-7.385	3.834	85.345	Pro158, Leu207, Tyr156	No ligand interaction atoms		
B3	-15.1	4.575	88.952	Glu155, Ala104, Ala157	No ligand interaction atoms		
B4	-18.603	4.122	89.321	Pro158, Leu207, Tyr156	No ligand interaction atoms		
B5	-20.06	3.719	91.378	Glu155, Ala104, Ala157	LYS106	B4:H28 - A: LYS106:CD B4:H28 - A: LYS106:HD2 B4:H25 - A: LEU207:HD11	2.144000 1.670000 1.805000
B6	-24.501	4.319	91.563	LEU207 Pro158, Leu207, Tyr156	LEU83	B5:H24 - A: LEU83:O B5:H24 - A: LEU83:C B5:H29 - A: LYS106:H22 B5:H25 - A: LEU207:HD21 B5:C13 - A: LEU207:HD21	1.971000 2.131000 1.721000 1.226000 1.928000
B7	-16.461	5.39	96.683	LEU83	LYS106	B6:H24 - A: LEU83:O B6:H24 - A: LEU83:C B6:H29 - A: LYS106:H22 B6:H25 - A: LEU207:HD21 B6:C13 - A: LEU207:HD21	1.910000 2.158000 1.583000 1.206000 2.031000
B8	-19.21	4.85	96.378	LEU207 Pro158, Leu207, Tyr156	LEU83	B7:C17 - A: ALA217:HB1 B7:C18 - A: LYS106:H22 B7:H27 - A: LEU207:HD21 B7:H35 - A: LYS106:HZ1	1.965000 2.206000 1.657000 1.516000
B9	-11.701	4.261	95.744	Glu155, Ala104, Ala157	LEU83	B8:H25 - A: LEU83:O B8:H25 - A: LEU83:C B8:H26 - A: LEU207:HD21 B8:H30 - A: LYS106:HD1	2.385000 2.212000 1.743000 1.819000
C1	12.93	4.427	98.927	LEU83	LYS106	B9:H25 - A: LEU83:O B9:H26 - A: LEU207:HD11 B9:H29 - A: LYS106:H22	2.456000 1.755000 1.533000
C2	3.409	4.307	104.36	LEU207 Pro158, Leu207, Tyr156	LEU83	C1:O14 - A: LEU207:HD21	1.783000
C3	0.596	3.584	104.05	Glu155, Ala104, Ala157	LEU83, LYS106	No Ligand interaction atoms	
C4	9.741	4.223	104.357	LEU207 Pro158, Leu207, Tyr156	LEU83	No Ligand interaction atoms	

(Contd...)

Table 2: (Continued)

Name	Electrostatic energy	Van der waals energy	LibDock score	Interacting aminoacids	Interacting atoms	h-bond distance
C5	7.965	3.419	104.186	LEU83 LYS106 LEU207 Pro158, Leu207, Tyr156 Glu155.Ala104, Ala157	No ligand interaction atoms	
C6	1.362	4.33	1\08.812	LEU83 LYS106 LEU207 Pro158, Leu207, Tyr156 Glu155.Ala104, Ala157	C6:H28 - A: LEU207:HD11 A: GLU161:HN - C6:O10	1.492000 2.483000
C7	10.734	3.997	108.285	LEU83 LYS106 LEU207 Pro158, Leu207, Tyr156 Glu155.Ala104, Ala157	C7:H26 - A: LEU207:HD11 C7:O14 - A: LEU207:HD21	1.713000 1.824000
C8	17.994	5.315	108.396	LEU83 LYS106 LEU207 Pro158, Leu207, Tyr156 Glu155.Ala104, Ala157	C8:C18 - A: GLY160:HA1 C8:H30 - A: TYR156:CE1	2.205000 1.866000
C9	19.317	4.366	\107.944	LEU83 LYS106 LEU207 Pro158, Leu207, Tyr156 Glu155.Ala104, Ala157	C9:O14 - A: LEU207:HD21 C9:H26 - A: LEU207:HD11	1.820000 1.776000
C10	14.912	5.467	108.156	LEU83 LYS106 LEU207 Pro158, Leu207, Tyr156 Glu155.Ala104, Ala157	C10:H30 - A: TYR156:CE1 C10:H30 - A: TYR156:HE1 C10:C18 - A: GLY160:HA1	2.067000 1.378000 2.204000
C11	13.427	4.974	112.523	LEU83 LYS106 LEU207 Pro158, Leu207, Tyr156 Glu155.Ala104, Ala157	A: ALA157:HN - C11:O10 A: LYS106:H22 - C11:O22 C11:H29 - A: LYS106:H22 C11:H32 - A: LEU207:HD21 C11:H32 - A: LEU207:CD2	1.957000 2.491000 1.084000 1.311000 2.112000
C12	3.479	2.699	93.263	LEU83 LYS106 LEU207 Pro158, Leu207, Tyr156 Glu155.Ala104, Ala157	A: LYS106:H22 - C12:O10 C12:N4 - A: LEU207:HD21	2.372000 1.825000
C13	-68.277	2.329	116.558	LEU83 LYS106 LEU207 Pro158, Leu207, Tyr156 Glu155.Ala104, Ala157	A: ALA157:HN - C13:O10 A: LYS106:H22 - C13:N15 A: LYS106:H21 - C13:O18 C13:H35 - A: LEU207:HD21 C13:C23 - A: LEU207:HD21 C13:H31 - A: LYS106:NZ C13:H31 - A: LYS106:H22	2.021000 2.284000 2.066000 1.813000 1.970000 1.979000 1.066000

standard analysis value like level 0 for human intestinal absorption, level 3 and level 4 for solubility, level 0 for non-inhibitory property with CYP450 2D6, level 3 for BBB penetration, and level 0 for non-toxicity were filtered for obtaining drug like compounds. Fig. 7 shows the plot of predicted values of drug absorption for our compounds. X-axis indicates the solubility of the compounds and Y-axis indicates the log p values. ADMET descriptors, the 2D polar surface area-2D in

A2 per compound is plotted against their consonant estimated atom-type partition coefficient (ALogP98). The space covered by the ellipse is a prophecy of excellent absorption without any violation of ADMET properties.

Ellipses indicate the absorption model at 95% and 99% confidence limit to the BBB and intestinal absorption models.

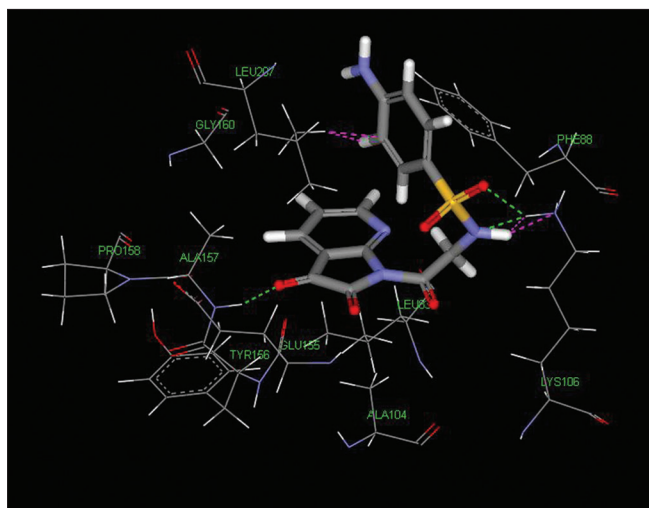


Fig. 4: Hydrogen bond interactions of compound C13 with human Aurora B Kinase

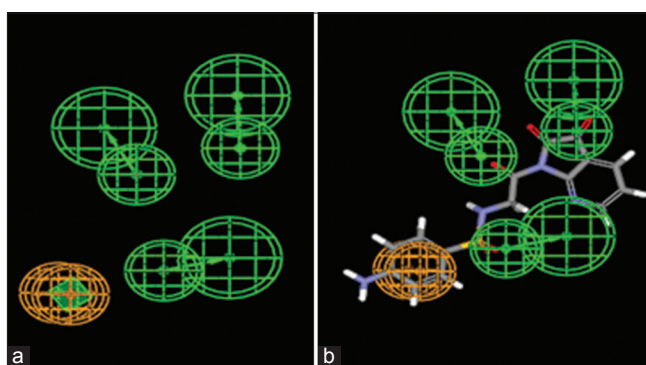


Fig. 5: (a) Generated common feature-based ligand pharmacophore model (hypothesis 1) showing the hydrogen bond acceptors (green) and the ring aromatic feature (orange), (b) alignment of the compound C13 on the common feature pharmacophore model

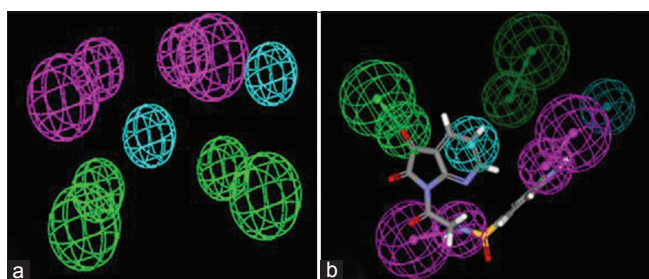


Fig. 6: (a) structure-based pharmacophore model of human Aurora B kinase, (b) mapping of high active compound C13 on to the pharmacophore model

CONCLUSION

In this study, the synthesized azaindole derivatives are examined for their anticancer activity against the targeted protein Aurora B kinase through docking studies. The docking results analyzed the important and specific interactions, which are important for describing the affinity of these ligand molecules toward the protein. In addition, the conducted pharmacophore studies revealed the critical chemical features of the ligand and structural features of the protein responsible for their protein-ligand complex binding. Furthermore, the ADMET properties

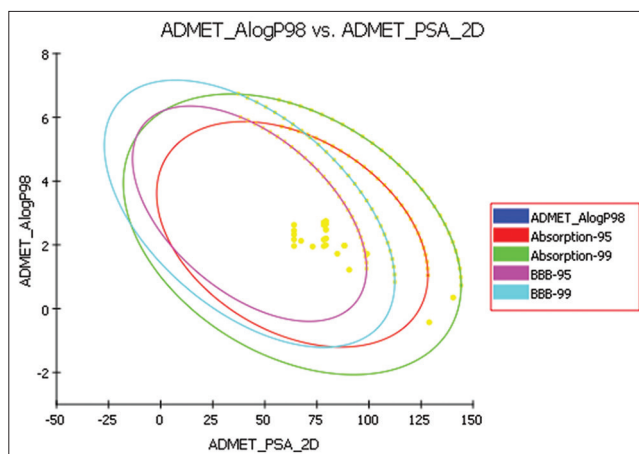


Fig. 7: Plot of polar surface area versus LogP for candidate compounds showing the 95% and 99% confidence limit ellipses corresponding to the blood-brain barrier and intestinal absorption models

Table 3: Features shared by the 10 hypotheses in the common feature pharmacophore model

Hypothesis	Feature	Rank	MaxFit
01	RAAA	266.453	4
02	RAAA	263.238	4
03	RAAA	262.038	4
04	RAAA	257.714	4
05	RAAA	256.747	4
06	RAAA	255.740	4
07	RAAA	252.218	4
08	RAAA	251.802	4
09	RAAA	250.133	4
10	HAAA	249.195	4

Table 4: Predicted fit values of compounds from the common feature-based hypothesis hypothesis 1

Name	Fit value	Pharmprint
A1	3.967	'1111'
A2	4	'1111'
A3	3.999	'1111'
A4	3.983	'1111'
A5	3.999	'1111'
B1	2.53	'1111'
B2	2.526	'1111'
B3	2.52	'1111'
B4	2.521	'1111'
B5	2.525	'1111'
B6	2.522	'1111'
B7	2.534	'1111'
B8	2.587	'1111'
B9	2.576	'1111'
C1	1.446	'1111'
C10	2.381	'1111'
C11	2.022	'1111'
C12	1.771	'1111'
C13	4.093	'1111'
C2	1.686	'1111'
C3	1.882	'1111'
C4	1.835	'1111'
C5	1.705	'1111'
C6	2.346	'1111'
C7	2.277	'1111'
C8	2.201	'1111'
C9	2.223	'1111'

Table 5: The predicted fit values of compounds from the structure-based pharmacophore model of human aurora B kinase

Name	Acceptor 13	Acceptor 9	Donor 28	Donor 49	Fit value	Hydrophobe 10	Hydrophobe 24	Pharmprint
C13	1	0	1	1	3.159	1	0	'011110'
C6	1	1	0	0	2.721	1	1	'110011'
C11	0	1	1	0	2.661	1	1	'101011'
C8	0	1	1	0	2.405	1	1	'101011'
C9	0	1	1	0	2.285	1	1	'101011'
A4	1	0	1	0	2.22	1	1	'011011'
C10	0	1	1	0	2.178	1	1	'101011'
C7	0	1	1	0	2.139	1	1	'101011'
B6	1	1	0	0	2.029	1	1	'110011'
C5	1	0	1	0	1.981	1	1	'011011'
B8	1	1	0	0	1.882	1	1	'110011'
C2	1	0	1	0	1.878	1	1	'011011'
C3	0	1	1	0	1.873	1	1	'101011'
C4	0	1	1	0	1.842	1	1	'101011'
C1	0	1	1	0	1.813	1	1	'101011'
A2	1	0	1	0	0.843	1	1	'011011'
A5	1	0	1	0	0.795	1	1	'011011'
A1	1	0	1	0	0.758	1	1	'011011'
A3	1	0	1	0	0.736	1	1	'011011'
C12	1	0	1	1	0.325	1	0	'011110'
B5	0	0	1	1	0.146	1	1	'001111'

Table 6: Predicted ADMET properties of the compounds

Name	BBB	Absorption	Solubility	Hepatotoxicity	CYP2D6	PPB
A1	3	0	3	1	0	2
A2	3	0	2	1	0	2
A3	3	0	3	1	0	2
A4	3	0	3	1	0	2
A5	3	0	2	1	0	2
B1	2	0	3	1	0	2
B2	3	0	3	1	0	2
B3	2	0	2	1	0	2
B4	2	0	3	1	0	2
B5	3	0	3	1	0	2
B6	3	0	3	1	0	2
B7	3	0	3	1	0	2
B8	3	0	3	1	0	2
B9	2	0	3	1	0	2
C1	3	0	3	1	1	2
C10	3	0	2	1	0	2
C11	3	0	3	1	0	2
C12	4	1	4	1	0	2
C13	4	1	3	1	0	2
C2	3	0	2	1	0	2
C3	3	0	3	1	0	2
C4	3	0	2	1	0	2
C5	3	0	3	1	0	2
C6	3	0	3	1	0	2
C7	3	0	3	1	0	2
C8	3	0	2	1	0	2
C9	3	0	3	1	0	2

ADMET: Absorption, distribution, metabolism, excretion and toxicity

of these compounds are reliable. Together, the results also provide evidence to show that the inhibitory effect of the azaindole derivatives against Aurora kinase, could aid in determining the lead molecules against cancer.

REFERENCES

- Andrews PD. Aurora kinases: Shining lights on the therapeutic horizon? *Oncogene* 2005;24(32):5005-15.
- Bolanos-Garcia VM. Aurora kinases. *Int J Biochem Cell Biol* 2005;37(8):1572-7.
- Katayama H, Sen S. Aurora kinase inhibitors as anticancer molecules. *Biochim Biophys Acta* 2010;1799(10-12):829-39.
- Hochegger H, Hégarat N, Pereira-Leal JB. Aurora at the pole and equator: Overlapping functions of Aurora kinases in the mitotic spindle. *Open Biol* 2013;3(3):120185.
- Dar AA, Goff LW, Majid S, Berlin J, El-Rifai W. Aurora kinase inhibitors – Rising stars in cancer therapeutics? *Mol Cancer Ther* 2010;9(2):268-78.
- Lens SM, Voest EE, Medema RH. Shared and separate functions of polo-like kinases and aurora kinases in cancer. *Nat Rev Cancer* 2010;10(12):825-41.
- Bischoff JR, Plowman GD. The Aurora/Ipl1p kinase family: Regulators of chromosome segregation and cytokinesis. *Trends Cell Biol* 1999;9(11):454-9.
- Fu J, Bian M, Jiang Q, Zhang C. Roles of Aurora kinases in mitosis and tumorigenesis. *Mol Cancer Res* 2007;5(1):1-10.
- Meraldi P, Honda R, Nigg EA. Aurora kinases link chromosome segregation and cell division to cancer susceptibility. *Curr Opin Genet Dev* 2004;14(1):29-36.
- Ke YW, Dou Z, Zhang J, Yao XB. Function and regulation of Aurora/Ipl1p kinase family in cell division. *Cell Res* 2003;13(2):69-81.
- Jayanthan A, Ruan Y, Truong TH, Narendran A. Aurora kinases as druggable targets in pediatric leukemia: Heterogeneity in target modulation activities and cytotoxicity by diverse novel therapeutic agents. *PLoS One* 2014;9(1):e102741.
- Keen N, Taylor S. Aurora-kinase inhibitors as anticancer agents. *Nat Rev Cancer* 2004;4(1):927-36.
- Ruchaud S, Carmena M, Earnshaw WC. Chromosomal passengers: Conducting cell division. *Nat Rev Mol Cell Biol* 2007;8(10):798-812.
- Kelly AE, Funabiki H. Correcting aberrant kinetochore microtubule attachments: An Aurora B-centric view. *Curr Opin Cell Biol* 2009;21(1):51-8.
- van der Waal MS, Hengeveld RC, van der Horst A, Lens SM. Cell division control by the Chromosomal Passenger Complex. *Exp Cell Res* 2012;318(12):1407-20.
- Cooke CA, Heck MM, Earnshaw WC. The inner centromere protein (INCENP) antigens: Movement from inner centromere to midbody during mitosis. *J Cell Biol* 1987;105:2053-67.
- Earnshaw WC, Bernat RL. Chromosomal passengers: Toward an integrated view of mitosis. *Chromosoma* 1991;100(3):139-46.
- Earnshaw WC, Cooke CA. Analysis of the distribution of the INCENPs throughout mitosis reveals the existence of a pathway of structural changes in the chromosomes during metaphase and early events in cleavage furrow formation. *J Cell Sci* 1991;98:443-61.
- Adams RR, Maiato H, Earnshaw WC, Carmena M. Essential roles of Drosophila inner centromere protein (INCENP) and aurora B in histone H3 phosphorylation, metaphase chromosome alignment, kinetochore disjunction, and chromosome segregation. *J Cell Biol* 2001;153(4):865-80.
- Carvalho A, Carmena M, Sambade C, Earnshaw WC, Wheatley SP. Survivin is required for stable checkpoint activation in taxol-treated HeLa cells. *J Cell Sci* 2003;116:2987-98.
- Honda R, Körner R, Nigg EA. Exploring the functional interactions

- between Aurora B, INCENP, and survivin in mitosis. Mol Biol Cell 2003;14(8):3325-41.
22. Gassmann R, Carvalho A, Henzing AJ, Ruchaud S, Hudson DF, Honda R, *et al.* Borealin: A novel chromosomal passenger required for stability of the bipolar mitotic spindle. J Cell Biol 2004;166(2):179-91.
 23. Vader G, Kauw JJ, Medema RH, Lens SM. Survivin mediates targeting of the chromosomal passenger complex to the centromere and midbody. EMBO Rep 2006;7(1):85-92.
 24. Bayliss R, Fry A, Haq T, Yeoh S. On the molecular mechanisms of mitotic kinase activation. Open Biol 2012;2(11):120136.